Snake-Inspired Kirigami Skin for Lateral Undulation of a Soft Snake Robot

Callie Branyan[®], Ross L. Hatton[®], and Yiğit Mengüç[®]

Abstract—Frictional anisotropy, as produced by the directionality of scales in snake skin, is necessary to propel snakes across flat, hard surfaces. This work illustrates the design, fabrication, and testing of a snake-inspired skin based on kirigami techniques that, when attached to a soft snake robot, improves the robot's locomotion capabilities when implementing a lateral undulation gait. Examination of snake scales in nature informed the shape and texture of the synthetic scales, which are activated through the buckling of kirigami lattices. Biological snakes have microornamentation on their scales, which is replicated by scoring ridges into the plastic skin. This microornamentation contributes to the lateral resistance necessary for lateral undulation. The skin's frictional properties were experimentally determined, as were their contributions to the locomotion of the robot across a flat, hard, textured surface. Contributions to locomotion from scale profile geometry, scale microornamentation, and scale angle of attack were identified. The range of longitudinal COF ratios was 1.0 to 3.0 and the range of lateral COF ratios was 0.9 to 3.3. The highest performing skin was the triangular scale profile with microornamentation, producing a velocity of 6 mm/s (0.03 BL/s) which is an increase of 335% over the robot with no skin when activated to maximum achievable curvature.

Index Terms—Soft robot materials and design, biologically-inspired robots, flexible robots.

I. INTRODUCTION

IMBLESS locomotion strategies couple the deformability of the organism's body and the frictional properties of the organism's skin to successfully locomote across a wide range of terrains. The relatively simple morphology of limbless organisms, and the versatility of their locomotion strategies make them well suited to navigate complex environments consisting of constrictive spaces, fluidic media, and obstacle ridden surfaces. Lateral undulation, the most common gait used by snakes, relies mostly on interactions with obstacles. As lateral bends of the

Manuscript received September 9, 2019; accepted January 9, 2020. Date of publication January 28, 2020; date of current version February 7, 2020. This letter was recommended for publication by Editor Kyu-Jin Cho upon evaluation of the Associate Editor and Reviewers' comments. This work was supported by the National Science Foundation (award IIS-1734627) and by the Office of Naval Research Young Investigator Program (ONR YIP N00014-16-1-2529; P.O. Tom McKenna). (Corresponding author: Callie Branyan.)

C. Branyan and R. L. Hatton are with Collaborative Robotics and Intelligent Systems Institute, Oregon State University, Corvallis, OR 97331, US (e-mail: branyanc@oregonstate.edu; ross.hatton@oregonstate.edu).

Y. Mengüç is with Collaborative Robotics and Intelligent Systems Institute, Oregon State University, Corvallis, OR 97331, US, and also with Facebook Reality Labs, Redmond, WA 98052, US (e-mail: yigit.menguc@oregonstate.edu).

This article has supplementary downloadable material available at https://ieeexplore.ieee.org, provided by the authors.

Digital Object Identifier 10.1109/LRA.2020.2969949

snake's body propagate down the backbone, these bends can brace against obstacles to push the snake forwards [1]. However, when obstacles are absent in the environment, significant displacement using lateral undulation depends on the interactions between the snake's scales and asperities on the terrain's surface [2].

The anisotropic properties of snake skin originate in the morphology and activation of their ventral scales. At the body level, snake skin exhibits longitudinal (along the backbone) anisotropy through the overlapping pattern of the scales allowing for smooth gliding forwards (with the scales) and resistance sliding backwards (against the scales). Snakes also exhibit high friction in the lateral axis (across the scales) that in combination with the deformation of their body can provide lateral resistance to push off against similar to pushing off an obstacle [3]. This can be represented as a lateral-longitudinal anisotropy which is the ratio between resistance across the scales and resistance when moving forwards with the scales. Close examination of snake skin revealed that at the micro level snake scales exhibit microornamentation (micro-ridges, nanoindentations, or fibular components), that may contribute the lateral resistance needed to traverse environments devoid of obstacles [4].

Many snake-inspired robots use wheels to provide the lateral resistance necessary for lateral undulation [5]–[7]. However, the addition of wheels limits the traversable terrains to hard, flat surfaces. There has been success in improving locomotion of a rigid snake robot with the addition of artificial scales to provide longitudinal anisotropy [8], but they did not examine friction in the lateral direction.

The skin developed in this work utilizes kirigami, a Japanese artform that involves cutting parallel lattices into a material, such that when it is uniaxially stretched, it produces out-of-plane buckling. The profile cut into the sheet, and the patterning of these profiles can be varied to alter the feature that pops out of plane (see Fig. 1(b)) [9]. Recently, kirigami has been used to develop skin for soft robots utilizing a rectilinear gait [10] and a two-anchor crawling gait [11], both of which involve the cycling of elongation and contraction of a soft actuator. However, a skin had not yet been developed for a snake-inspired robot using a lateral undulation gait, which introduces novel skin mechanics – such as asymmetric buckling and gradients of strain.

In this work, a snake-inspired skin that provides the advantages of frictional anisotropy without interfering with the deformation required to propagate bends along the soft robot's body was designed and implemented on a soft robot. Using kirigami allowed for the activation and deactivation of scales as the soft actuators deform – similar to biological snakes activating their scales to increase friction [12]. To produce lateral resistance, micro-ridges, a common form of microornamentation in nature, were implemented by scoring polyester plastic sheets along

2377-3766 © 2020 IEEE. Personal use is permitted, but republication/redistribution requires IEEE permission. See https://www.ieee.org/publications/rights/index.html for more information.

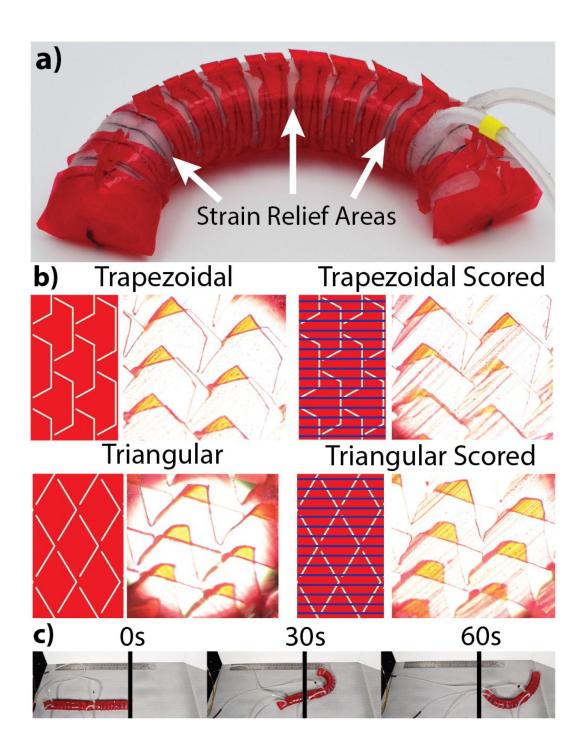


Fig. 1. (a) Strain relief areas allow for curvature of soft actuator. (b) Kirigami scale profile geometries and microornamentation. (c) Locomotion of soft snake robot with skin.

the longitudinal axis. We propose that these ridges provide more resistance laterally than a smooth version of the same skin. The coefficients of friction (COF) of the snake-inspired skin were experimentally determined and the corresponding anisotropic ratios were calculated. The scale profile geometry, and scale microornamentation were varied to measure their contributions to the robot's locomotion capabilities. The angle of attack (AOA) of the scales coupled to the curvature of the robot's actuators was also examined for contributions to the frictional properties of the robot, and locomotion in general.

The design and fabrication of the skins are outlined in Section II, the experiments for characterizing the frictional properties of the skin are illustrated in Section III, the results of the subsequent locomotion studies are presented in Section IV, and finally, the contributions from the skin, and potential future directions are discussed in Section V.

II. DESIGN AND FABRICATION

The soft snake robot, described previously in [13], consisted of two silicone rubber (EcoFlex 00–30), pneumatic actuators 100 mm long with an elliptical cross-section with a semi-major axis of 24 mm and a semi-minor axis of 14 mm. A woven fiberglass, strain-limiting layer was embedded between the two air chambers to produce bidirectional bending with no extension. Two actuators were combined in series to enable the propagation of bending waves down the backbone of the robot, inspired by the lateral undulation gait used by many terrestrial snakes. The fabrication processes for implementing microornamentation, and wrapping the skin around the soft actuator are shown in Fig. 2. The skin consisted of a lattice pattern, originally developed in [10], cut into polyester plastic sheets (AccuTrex Products Inc., PA) with a thickness of 51 μ m using a knife plotter (Silhouette Cameo 3). Two shape profiles, triangular and



Fig. 2. Fabrication processes for preparing skin and wrapping around an actuator

trapezoidal, were selected based on previous high coefficient of friction results [10]. Microornamentation was implemented by scoring ridges into the plastic sheets before cutting the scale pattern. The ridges were plastically deformed into the sheets using a scoring board (EK Tools) with score lines 1.25 mm wide and 1.25 mm deep with 1 mm spacing.

Kirigami patterns produce out-of-plane deformation when a uniaxial strain is applied across the lattice. An extending actuator is ideal for producing uniaxial strain, however, actuators that can only extend cannot produce lateral undulation. Previous skins were for extending actuators and do not allow for curvature as they restrict the biaxial deformability of a bending actuator [10]. Bending was enabled by introducing strain relief along the length of the skin (see Fig. 1(a)). To promote consistent activation of the scales, these areas of strain relief had to be relatively small, and embedded uniformly along the skin.

To further promote bending, the "spine," which adheres the skin to itself when wrapped around the actuator, needed to be adhered out-of-plane from the strain and separated at the strain relief areas to allow the skin to slide along the actuator and prevent the spine from pulling apart due to shearing. To fully contain the soft actuator, the plastic sheet was cut to reduce creases at the ends of the elliptical body, and adhered (SuperGlue Gorilla Glue) to the plastic on the body of the actuator. The tubing for air supply was fed through the closest strain relief area. The actuators were adhered to one another using SilPoxy placed on the capped ends and allowed to cure.

Fig. 3 shows the relationship between pressure and curvature to illustrate how the strain relief design allowed for more curvature of the actuator. The four skins tested in this work are compared to an actuator with no skin, and actuators with no strain relief design. The characterization shows that the skin does restrict curvature as expected, but can still reach moderate curvatures. The actuators without strain relief take larger pressures to reach their maximum curvatures. The maximum

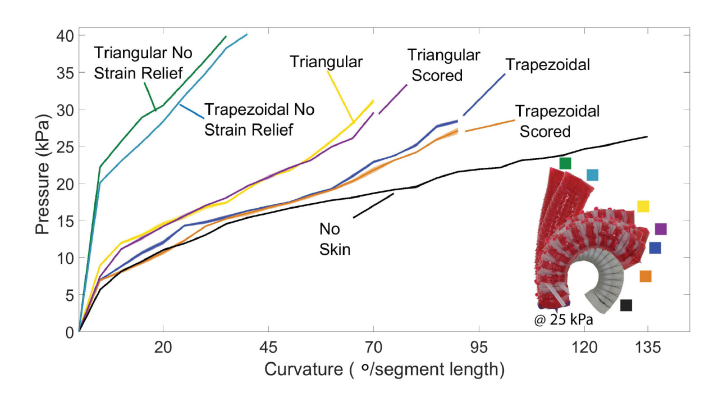


Fig. 3. Effect of strain relief designs on curvature vs. pressure relationship. Inset shows the achievable curvature of each skin when the actuator is inflated to the same pressure.

curvature achieved by the trapezoidal profile actuators before failure was 90° and for the triangular profile actuators was 70° . At higher curvatures, the plastic skin would rip along the hinges as the plastic skin drew tighter around the elastomeric body of the actuator. The effects of microornamentation on the relationship between pressure and curvature are negligible within the scope of this work. A maximum curvature of 60° was used to ensure all experiments were performed consistently without inducing failure of the actuators.

When the actuators bend, the local interaction between the skin and the soft body produced a strain on the lattice causing out-of-plane buckling. Strain was measured at the center line along the bottom of the actuator as that is the area of highest engagement when the skin is in contact with the terrain. The triangular skin was stiffer than the trapezoidal which is why it took a higher pressure to produce the same curvature. Therefore, at each curvature the triangular skin had a lower achieved strain.

III. CHARACTERIZATION OF FRICTIONAL PROPERTIES

To determine how the frictional properties of the skin were contributing to locomotion, the coefficient of friction (COF), dependent on the angle of attack (AOA) of the scales, for each skin needed to be characterized. The scales pop out when a strain is applied to the skin. The strain is applied through the bending of the actuator meaning the AOA of the scales is determined by how much the actuators bend. Therefore, before the COF of the skin could be measured, the relationship between the curvature of the actuator and the resulting AOA of the scales needed to be characterized.

A. Characterizing Angle of Attack

The curvature-AOA relationship was characterized by inflating a skin-wrapped actuator to different curvatures and measuring the resulting AOA of the scales. The trend in Fig. 4 shows that as curvature, and therefore strain increased, AOA increased. Microornamentation had no impact on the AOA. There was a difference in achievable AOA across scale profile geometries as the triangular profile was stiffer than the trapezoidal profile, and therefore produced a lower strain on the skin. The plot in Fig. 4 has two axes for strain to show that at the same curvature, different strains were measured.

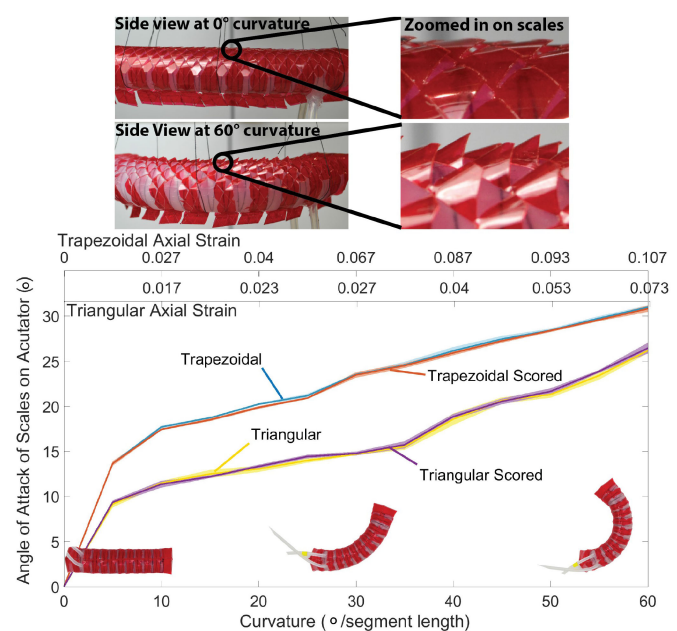


Fig. 4. Experimentally determined relationship between curvature of the actuator and the resulting AOA.

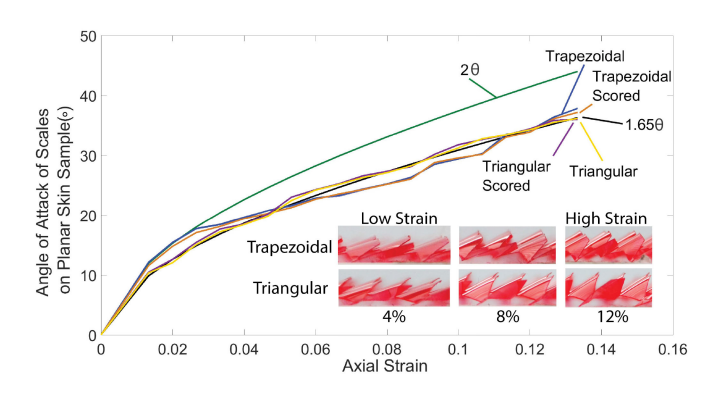


Fig. 5. Planar AOA measurements from the four types of skin compared to the model shown in Equation 1.

When the skin was wrapped around the elliptical actuator, the scales' orientation changed depending on their position along the circumference, as well as changing when the actuator was at different curvatures. Therefore, a characterization, and testing of a planar skin sample was used as a baseline to ensure all scales had the same orientation perpendicular to surface asperities. Characterization of the AOA of the scales on a planar sample can be seen in Fig. 5. A geometric model for the opening angle of a commonly-used kirigami lattice with a pattern of linear cuts [14]–[17] has been previously derived, but not experimentally validated [14]. The model,

$$2\theta(\epsilon_x) = \arccos\left[\sin\left(2\arccos\frac{1+\epsilon_x}{\sqrt{2}}\right) + \tan\left(\frac{\pi}{4} + \arccos\frac{1+\epsilon_x}{\sqrt{2}} - \arccos\frac{1+\epsilon_x}{\sqrt{2}}\right)\right],$$
(1)

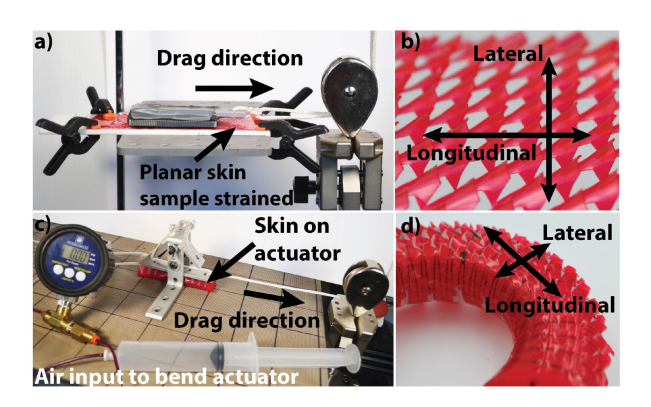


Fig. 6. Apparatus for measuring the COF of planar skin samples (a), and for skin on actuator (c). Drag directions of planar skin samples (b). and of actuators with skin (d).

represents the opening angle of the pop-out structure as 2θ , and is a function of the applied uniaxial strain, ϵ_x .

The function, plotted as 2θ in Fig. 5, has the right shape as the observed experimental data, in that the angle increases with increasing strain at a decreasing rate, but was overestimating the AOAs measured. This is likely due to the model being derived for a linear cut pattern which produces out-of-plane buckling up and down. The patterns used in this work only have one direction of out-of-plane buckling. They also have different cut profiles which could be contributing to the reduction of AOA as well. Since the function has the right shape, we can include a scalar multiplier to better fit the experimental data. The new function, represented as 1.65θ in Fig. 5), was produced by multiplying the function described in Equation 1 by a scalar value of 0.825. It closely approximates the triangular profile relationship between strain and AOA. Examining the stress at the hinges upon uniaxial loading was outside the scope of this work, but could be used to identify why the original model does not accurately represent the magnitude of AOA.

B. Measuring the Coefficients of Friction

The COFs of the skin were characterized to determine the effects of scale profile, microornamentation, and angle of attack on locomotion. The frictional properties of the four skins were measured both in the planar case, where a skin sample was stretched to different strains, and in the curved case, where the skin was wrapped around the actuator and strained by the deformation of the actuator. These two cases were selected to determine if the curvature of the actuator, as well as the orientation of the scales interacting with asperities, had an effect on the COFs measured.

The planar case was tested by stretching a sample of each skin, and dragging a weighted surface sample across the scales (see Fig. 6(a)). The samples were stretched to different strains to produce an AOA corresponding to the AOAs measured at the selected curvatures. The curved case was tested by inflating the actuators to the selected curvatures, and dragging them across the surface (see Fig. 6(c)). A force profile was recorded using a Mark10 and 10 N load cell. The skins were tested in 3 configurations to determine the ratio of anisotropy; forwards (with the scales), backwards (against the scales), and laterally

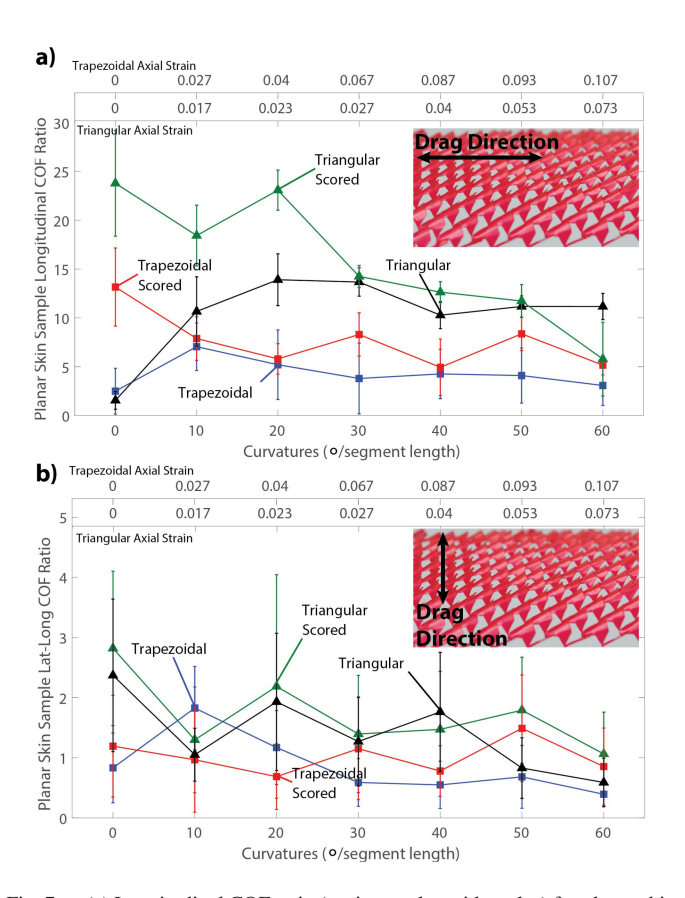


Fig. 7. (a) Longitudinal COF ratio (against scales: with scales) for planar skin sample. (b) Lateral-longitudinal COF ratio (across scales: with scales) for planar skin sample.

(across the scales) (see Fig. 6(b) and (d)). The effective COFs,

$$\mu_f = \frac{\left\langle F_f \right\rangle}{F_N}, \quad \mu_b = \frac{\left\langle F_b \right\rangle}{F_N}, \quad \mu_l = \frac{\left\langle F_l \right\rangle}{F_N}, \quad (2)$$

were calculated using the average frictional force $\langle F \rangle$ and the weight of the dragging apparatus/actuator F_N (1.7 N for actuator tests and 1.2 N for planar tests). The anisotropic friction ratios are defined as μ_b/μ_f for the longitudinal ratio, and μ_l/μ_f for the lateral-longitudinal ratio.

The results of the anisotropic friction ratios for the planar skin samples are plotted in Fig. 7. The x-axis is shown in terms of curvature because curvature is the controlled parameter during locomotion. In the planar case, the skin was strained to match the AOA measured at those curvatures. The triangular skin produced higher frictional coefficients, likely caused by the higher stiffness of the kirigami lattice. The friction ratio at the highest strain, and therefore highest AOA, is lower than at some of the lower to mid-range curvatures. At low to mid-range AOAs, the scales are less stiff, and flex backwards while interlocked with the asperity, increasing the area in contact with the asperity. At higher AOAs the scales are stiffer, and upon empirical examination during testing, have a weaker interaction with surface asperities. Further investigation is required to interrogate this interaction, as the micro-mechanics of skin-surface interactions were outside the scope of this work.

The anisotropic friction ratios for the skin on actuators are shown in Fig. 8. Again, at the highest curvature, and therefore

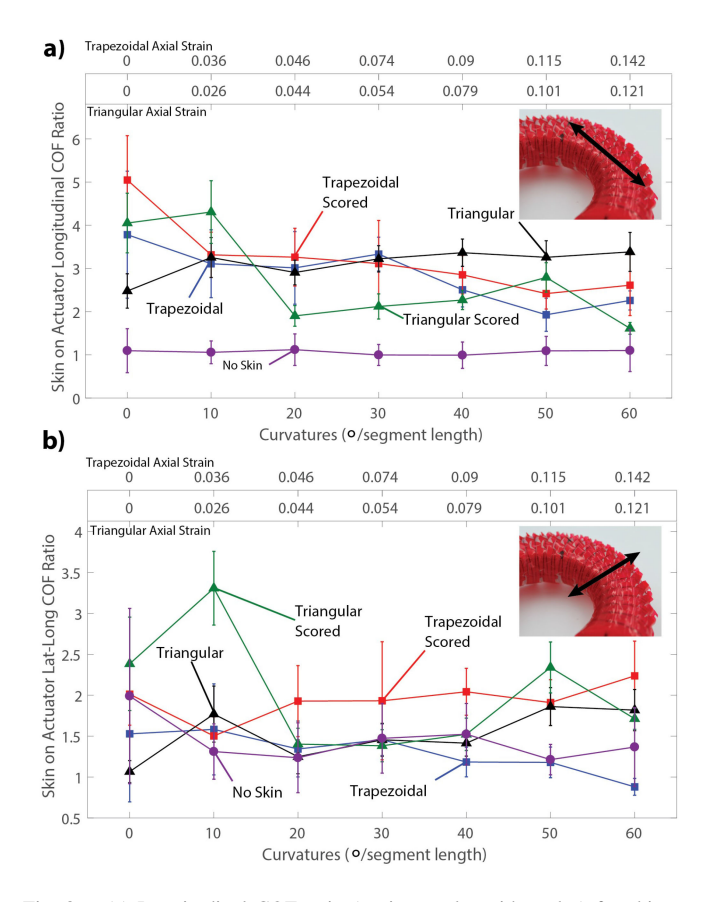


Fig. 8. (a) Longitudinal COF ratio (against scales:with scales) for skin on actuator. (b) Lateral-longitudinal COF ratio (across scales:with scales) for skin on actuator.

highest AOA, the longitudinal ratio is lower compared to midrange curvatures for most of the skins. The lateral-longitudinal ratio at the highest curvature is maximized for most of the skins. This is likely due to the scales being oriented over a range of angles relative to the asperities, increasing the number of scales interlocking, or partially interlocking with the asperity.

Figs. 7 and 8 show that microornamentation had an effect on both anisotropic ratios. At the majority of curvatures, the lateral-longitudinal anisotropy is increased by the presence of microornamentation. However, it also increases the longitudinal anisotropy. The ridges plastically deformed into the skin increase the longitudinal stiffness of the scales similar to how paper is stiffer when there are folds present.

The frictional anisotropy of terrestrial snakes has been widely studied across different species and testing surfaces, resulting in a range of ratios. From the literature, the ranges were: 1.0 to 3.0 for the longitudinal anisotropic ratio, and 0.99 to 1.46 for the lateral-longitudinal anisotropic ratio [2], [3], [18]–[20]. For all four kirigami skins, the range for the longitudinal anisotropic ratios was 1.9 to 5.1. The range of the lateral-longitudinal anisotropic ratios was 0.9 to 3.3. Therefore, we have successfully developed a snake-inspired skin with similar frictional properties as observed in nature.

IV. LOCOMOTION STUDIES

The main objective of this work was to improve the locomotion of the soft snake robot as it traversed a flat, textured surface

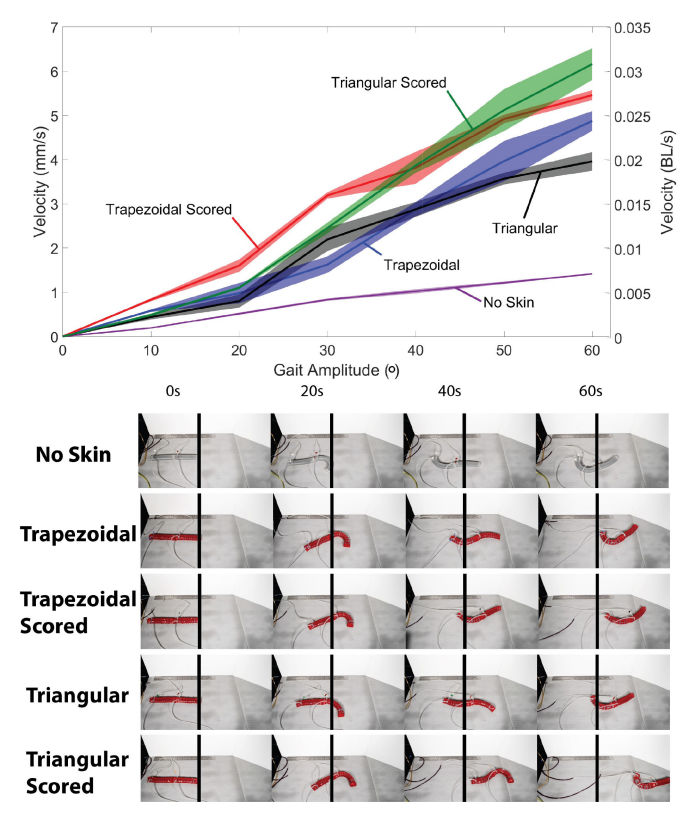


Fig. 9. Velocity of soft robot using a lateral undulation gait comparing the four types of skin to a robot with no skin.

utilizing the frictional strategies seen on biological snakes. All four skins were tested using a lateral undulation gait, varying only the amplitude of the curvature waves. Due to the coupling between actuator deformation and scale AOA, the AOA would change depending on the driven curvature, which alters the frictional properties of the robot. All robots, at curvatures from 10° to 60° in 10° increments, were tested on top of a metal block covered in a woven fiberglass mesh with an 18x16 mesh size and a 0.011" wire diameter (McMaster-Carr, 1017A87). Displacement data was collected using an OptiTrack Prime 13 motion capture system and used to calculate the velocity of each robot. A robot with no skin was tested as a control case to compare against each skin.

The results of the locomotion study are presented in Fig. 9. As in [13], all five robots achieved their maximum displacement per cycle (and thus maximum speed for a fixed cycle time) in the gaits with the maximum achievable curvature amplitude—i.e., the robots' bending limits were reached before increasing the bending amplitude became detrimental to performance.

The scored skin on both scale profile geometries outperformed their smooth counterparts. All skins significantly improved velocity of the robot when compared to a robot with no skin, which produced some displacement likely caused by adhesion during surface interactions. The highest performing skin, triangular profile with microornamentation, improved the velocity of the robot with no skin by 335% and improved the velocity of the robot with the triangular profile with no microornamentation by 55%. The trapezoidal skin with microornamentation improved velocity of the robot with no skin by 285% and improved velocity of the trapezoidal profile with no microornamentation by 10%.

Beyond our observation that scored skins outperformed unscored skins, and that both provided significantly better performance than no skin, we were not able to identify a clear correlation between the measured COFs and the locomotive performance. Further investigation of this correlation will require a better understanding of how variations in the COFs at different parts of the gait (as the scales are activated and deactivated across the body) and of the role that the longitudinal COF ratio plays in undulatory motion, both at the system level and at the level of individual scales. For example, as the actuator curves more, it reduces the number of scales ideally interacting with asperities as the robot pushes forwards, but as the robot pushes laterally, there are more scales interlocking with asperities.

V. CONCLUSION

In summary, we have shown that a kirigami skin can be developed to improve the locomotion capabilities of a soft snake robot using a lateral undulation gait. Though kirigami has been used previously to show how directional frictional properties can improve locomotion, it has not been used for a gait that requires significant lateral deformation as seen in snake gaits. By introducing areas of strain relief along the length of the skin, significant curvature can be achieved while still maintaining the strain required to produce the out-of-plane buckling that is characteristic of kirigami.

Microornamentation was included for the first time for a snake-inspired skin. It was introduced through the scoring of the polyester plastic material which produced permanent ridges along the longitudinal axis of the skin. Inspired by snakes in nature, microornamentation is proposed to increase lateral-longitudinal frictional anisotropy that provides the lateral resistance required to successfully produce lateral undulation. The experiments performed in this work show that the inclusion of microornamentation increased the lateral-longitudinal ratio of frictional anisotropy and improved the locomotion capabilities of the subsequent robot.

This initial work focused on the overall performance of the skin on the actuator and how the coupling of these systems contributed to improvements in locomotion. Future work can start to decouple some of the parameters observed during testing to further optimize the skin. Only one type of microornamentation was implemented, so further optimization on increasing lateral resistance can be explored by varying the micro-structures, as well as a more precise investigation of the contributed shear forces. Finally, the decoupling of the AOA of the scales and the deformation of the robot would be ideal. Ultimately, the kirigami skins presented here are a new and accessible method for introducing frictional anisotropy to a broad class of soft robots.

REFERENCES

- [1] C. Gans, "Terrestrial locomotion without limbs," *Amer. Zoologist*, vol. 2, pp. 167–182, 1962.
- [2] D. L. Hu, J. Nirody, T. Scott, and M. J. Shelley, "The mechanics of slithering locomotion," *Proc. Nat. Acad. Sci.*, vol. 106, no. 25, pp. 10 081–10 085, 2009.
- [3] H. A. Abdel-Aal, "On surface structure and friction regulation in reptilian limbless locomotion," *J. Mech. Behav. Biomed. Mater.*, vol. 22, pp. 115– 135, Jun. 2013.
- [4] M.-C. G. Klein and S. N. Gorb, "Epidermis architecture and material properties of the skin of four snake species," *J. Royal Soc.*, 2012. [Online]. Available: http://rsif.royalsocietypublishing.org/??
- [5] K. Y. Pettersen, "Snake robots R," Annu. Rev. Control, vol. 44, pp. 19–44, 2017. [Online]. Available: https://doi.org/10.1016/j.arcontrol.2017.09.006
- [6] C. D. Onal and D. Rus, "Autonomous undulatory serpentine locomotion utilizing body dynamics of a fluidic soft robot," *Bioinspiration Biomimetics*, vol. 8, pp. 26 003–10, 2013.
- [7] S. Hirose, Biologically Inspired Robots (snake-like locomotor and manipulator), London, U.K.: Oxford Univ. Press, 1993.
- [8] M. M. Serrano, A. H. Chang, G. Zhang, and P. A. Vela, "Incorporating frictional anisotropy in the design of a robotic snake through the exploitation of scales," in *Proc. IEEE Int. Conf. Robot. Autom.*, 2015, pp. 3729– 3734.
- [9] T. Castle et al., "Making the Cut: Lattice Kirigami Rules," Phys. Review Letters, vol. 113, no. 24, 2014, Art. no. 245502.
- [10] A. Rafsanjani, Y. Zhang, B. Liu, S. M. Rubinstein, and K. Bertoldi, "Kirigami skins make a simple soft actuator crawl," *Sci. Robot.*, vol. 3, no. 15, 2018, Art. no. eaar7555.
- [11] B. Liu, Y. Ozkan-Aydin, D. I. Goldman, and F. L. Hammond Iii, "Kirigami skin improves soft earthworm robot anchoring and locomotion under cohesive soil," in *Proc. IEEE Int. Conf. Soft Robot.*, 2019, pp. 828–833.
- [12] H. Marvi, J. P. Cook, J. L. Streator, and D. L. Hu, "Snakes move their scales to increase friction," *Biotribology*, vol. 5, pp. 52–60, 2016.
- [13] C. Branyan and Y. Menguc, "Soft Snake Robots: Investigating the Effects of Gait Parameters on Locomotion in Complex Terrains," in *Proc. IEEE/RSJ Int. Conf. Intell. Robots Syst.*, 2018, pp. 1–9. [Online]. Available: https://ieeexplore.ieee.org/document/8593404/
- [14] A. Rafsanjani, K. Bertoldi, and J. A. Paulson, "Buckling-Induced Kirigami," *Physical Rev. Lett.*, vol. 118, no. 8, 2017. [Online]. Available: https://journals.aps.org/prl/pdf/10.1103/PhysRevLett.118.084301
- [15] T. C. Shyu et al., "A kirigami approach to engineering elasticity in nanocomposites through patterned defects," *Nature Mater.*, vol. 14, no. 8, pp. 785–789, 2015.
- [16] A. Lamoureux, K. Lee, M. Shlian, S. R. Forrest, and M. Shtein, "Dynamic kirigami structures for integrated solar tracking," *Nature Commun.*, vol. 6, 2015, Art. no. 8092.
- [17] M. Isobe and K. Okumura, "Initial rigid response and softening transition of highly stretchable kirigami sheet materials," *Scientific Reports*, vol. 6, no. 1, 2016, Art. no. 24758.
- [18] J. Gray and H. W. Lissmann, "The Kinetics of Locomotion of the Grass-Snake," J. Exp. Biol., vol. 26, no. 4, pp. 354–367, 1950.
- [19] Berthe R. A., G. Westhoff, Bleckmann H., and Gorb S N, "Surface structure and frictional properties of the skin of the Amazon tree boa Corallus hortulanus (Squamata, Boidae)," J. Comparative Physiol. A, vol. 195, no. 3, pp. 311–318, 2009. [Online]. Available: https://doi.org/10.1007/s00359-008-0408-1
- [20] M. J. Baum, A. E. Kovalev, J. Michels, and S. N. Gorb, "Anisotropic friction of the ventral scales in the snake lampropeltis getula californiae," *Tribology Lett.*, vol. 54, no. 2, pp. 139–150, 2014.